Shiga toxin B subunits induce VWF secretion by human endothelial cells and thrombotic microangiopathy in ADAMTS13-deficient mice

Jing Huang,[1] David G. Motto,[2] David R. Bundle,[3] and J. Evan Sadler[1]

[1]Departments of Medicine, Biochemistry, and Molecular Biophysics, Washington University School of Medicine, St Louis, MO; [2]Department of Internal Medicine and Pediatrics, University of Iowa, Iowa City, IA; and [3]Department of Chemistry, University of Alberta, Edmonton, AB

Diarrhea–associated hemolytic uremic syndrome (D+HUS) is the most common cause of acute renal failure among children. Renal damage in D+HUS is caused by Shiga toxin (Stx), which is elaborated by *Shigella dysenteriae* and certain strains of *Escherichia coli*, in North America principally *E coli* O157:H7. Recent studies demonstrate that Stx also induces von Willebrand factor (VWF) secretion by human endothelial cells and causes thrombotic thrombocytopenic purpura, a disease with similarities to D+HUS, in *Adamts13*−/− mice. Stx occurs in 2 variants, Stx1 and Stx2, each of which is composed of 1 catalytically active A subunit that is responsible for cytotoxicity, and 5 identical B subunits that mediate binding to cell-surface globotriaosylceramide. We now report that B subunits from Stx1 or Stx2 can stimulate the acute secretion of VWF in the absence of the cytotoxic A subunit. This rapid effect requires binding and clustering of globotriaosylceramide, and depends on plasma membrane cholesterol and caveolin-1 but not clathrin. Furthermore, similar to Stx2 holotoxin, the isolated Stx2B subunits induce thrombotic microangiopathy in *Adamts13*−/− mice. These results demonstrate the existence of a novel Stx B-induced lipid raft–dependent signaling pathway in endothelial cells that may be responsible for some of the biological effects attributed previously to the cytotoxic Stx A subunit. (*Blood*. 2010;116(18):3653-3659)

Introduction

Shiga toxin–producing *E coli* (STEC) are responsible for a life-threatening food borne illness consisting of bloody diarrhea that may develop into the hemolytic uremic syndrome (HUS), which is characterized histologically by glomerular microvascular platelet adhesion/aggregation and fibrin polymer formation. Classic clinical features of diarrhea-associated HUS (D+HUS) include acute renal failure, thrombocytopenia, and microangiopathic hemolytic anemia. D+HUS is the most common cause of renal failure in children in the United States and is fatal in approximately 3%-5% of cases.[1,2]

STEC produce 2 main serogroups of Shiga toxins, Stx1 and Stx2. Shiga toxins (Stx) are complex holotoxins with an AB$_5$ structure. The active subunit (A) has N-glycosidase activity that cleaves the adenine from position 4324 of the 28S rRNA of the 60S ribosomal subunit. The B subunits form a noncovalently linked pentamer that mediates toxin attachment to membrane globotriaosylceramide receptors (Gb3 or CD77). After receptor binding and internalization, Stx travel in a retrograde direction through early/recycling endosomes to the trans-Golgi network, Golgi apparatus, and endoplasmic reticulum (ER). The toxins are transported across the ER membrane to the cytosol where the A subunit cleaves adenine 4324 from the 28S rRNA of the 60S ribosomal subunit, inhibiting protein synthesis and initiating a cascade of reactions termed the ribotoxic stress response, which ultimately leads to cell death.[3] It is worth noting that at least a few hours are required before these effects occur.

Recently, Nolasco and colleagues[4] reported that human umbilical vein endothelial cells (HUVECs) and human glomerular microvascular endothelial cells (HGMECs) secreted large amount of ultralarge von Willebrand factor (VWF) after treatment with Stx1 or Stx2 holotoxins. The amount of VWF secreted in response to 1-10nM Stx was comparable to that released by 0.1-20mM histamine. VWF secretion occurred within 10 minutes, which appears to be too fast to attribute to the ribotoxic stress response. In addition, challenge of *Adamts13*−/− mice with Stx causes systemic microvascular thrombosis that resembles human thrombotic thrombocytopenic purpura,[5] and the absence of VWF completely protects against Stx-induced thrombocytopenia and death.[6] Whether these responses require the catalytically active Stx A subunit was not assessed.

We now find that pentameric B subunits of Stx are sufficient to induce acute secretion of ultralarge VWF from cultured human endothelial cells and cause thrombotic microangiopathy in a disintegrin and metalloproteinase with thrombospondin type 1 motif, member 13 (ADAMTS13)–deficient mice. These activities are independent of the ribotoxic effect of Stx A subunits. Binding and clustering of Gb3 receptor is necessary but not sufficient for Stx B-induced VWF secretion. In addition, Gb3 localization in membrane rafts is required. These results uncover a previously unsuspected mechanism for Stx to cause endothelial activation and VWF-dependent thrombosis, which may contribute to the progression of D+HUS.

Methods

Plasmids encoding Stx1B in the pT7B5-1 vector[7] and Stx2B in the pET101 vector (Invitrogen), as well as rabbit polyclonal antibody against

Stx1B[8] were provided by Dr David B. Haslam (Washington University School of Medicine). Mouse monoclonal anti-Stx2B antibody 5H8[9] was obtained from Dr Saul Tzipori (Tufts University). HUVECs were from Lonza and cultured in medium EGM-2 (no. CC-3162). HGMECs were from Cell Systems and cultured in serum-containing medium (no. 4Z0-500). Stx1 and Stx2 holotoxins, recombinant cholera toxin B5 (CtxB), and goat anti-CtxB antibody were from List Biologicals. Some experiments were performed with recombinant Stx1B or Stx2B that have carboxyl-terminal His$_6$ tags (BEI Resources). Anti-CD77 IgM (clone 5B5) and mouse monoclonal anti–human caveolin-1 antibody were from BD Biosciences.

Expression and purification of recombinant pentameric Stx1B and Stx2B

The W34A mutation was introduced into Stx1B construct using a Quick-Change XL site-directed mutagenesis kit (Stratagene) and the following primers: 5′-GAATTATTCACCAACAGAGCGAATCTTCAGTCTC-3′ and 5′-GAGACTGAAGATTCGCTCTGTTGGTGAATAATTC-3′.

Plasmids encoding Stx1B (wild-type or W34A mutant) or Stx2B were transformed into competent *E coli* BL21. Protein expression was induced with 1mM IPTG when the OD$_{600}$ of 1-L bacteria culture (in LB+Ampicillin) reached 0.6. After 3 hours of induction, cells were collected by centrifugation and gently resuspended in 50 mL of sucrose solution (20% sucrose, 5mM EDTA [ethylenediaminetetraacetic acid], 20mM Tris-Cl, pH 8). Cells were incubated with sucrose solution for 20 minutes, centrifuged, and supernatants were discarded. Cell pellets were resuspended in ice-cold 5mM MgCl$_2$, incubated with gentle rocking for 15 minutes, and centrifuged again. The supernatants are periplasmic extracts that contain recombinant StxB proteins.

Periplasmic extracts were adjusted to contain 10mM imidazole, 300mM NaCl, and 50mM sodium phosphate, pH 7.4. Purification over His-Pur Cobalt column (Pierce) was conducted according to manufacturer's instructions. Eluted proteins were concentrated using Amicon ultrafiltration units (Millipore) with 10 000 molecular weight cutoff membranes. Imidazole was removed using Zebra desalting columns (Pierce). Protein preparations were then applied on a TSK G3000SW gel filtration column (Sigma-Aldrich) to determine their multimeric states, using purified BSA as a standard. Stx1B, Stx1B W34A, and Stx2B eluted near the position of ovalbumin (44 kDa), confirming that the preparations consisted mainly of pentamers.

Endotoxin (lipopolysaccharide, LPS) was removed with Detoxi-Gel endotoxin removal columns (Pierce) according to manufacturer's instructions. Levels of endotoxin before and after treatment were measured using a QCL-1000 Chromogenic Limulus Amebocyte Lysate End Point Assay kit (Lonza). After endotoxin removal, the residual endotoxin concentration was below 1 ng/mg of recombinant protein. Stx protein concentrations were measured with a Coomassie Plus Protein assay (Pierce) standardized with bovine serum albumin (BSA).

Quantitation of VWF strings or platelet-VWF complexes

Perfusion assays were performed in parallel plate flow chambers (Glycotech). as described previously.[10] Briefly, HUVECs were grown to a confluent monolayer on collagen coated glass coverslips. Alexa Fluor 594 conjugated polyclonal rabbit anti–human VWF antibody was used to detect VWF strings. Unless otherwise noted, perfusion buffer was medium 199 that contained CaCl$_2$ and MgCl$_2$, supplemented with 2% BSA, and the flow rate was adjusted with a syringe pump (Harvard Apparatus) to achieve a fluid shear stress of 2.5 dyn/cm^2. Images (10 fields) were collected after 10 minutes using an Axiovert 200M inverted microscope with a 40× objective, standard filter sets, a charge-coupled device camera, and Axiovision software Version 4 (Carl Zeiss). Fluorescent VWF strings in each field (magnification ×400) were counted, excluding strings shorter than 20 μm in length.

Confluent HGMECs (Cell Systems) on 35-mm dishes were perfused at 2.5 dyn/cm^2 with Stx variants and fixed platelets (Helena Laboratory) at 1×10^8/mL. After 5 minutes, images from 10 fields were acquired and adherent platelets were counted. Differences between mean values were assessed for significance using the Student *t* test.

Cell-surface VWF ELISA

Confluent HUVECs in 24-well plates were serum starved 1 hour, stimulated with Stx1B or Stx2B in quadruplicate for 30 minutes at 37°C, washed with PBS, fixed 10 minutes with 2% paraformaldehyde, and blocked 30 minutes with 2% BSA in PBS. Cell-surface VWF was detected with rabbit polyclonal horseradish peroxidase–anti-VWF antibody (P226; DAKO North America), diluted 1:10 000 for 45 minutes. After washing, horseradish peroxidase was detected with a TMB (3,3′,5,5′-tetramethylbenzidine) substrate kit (Pierce). After stop solution was added, supernatants were transferred to 96-well plates and optical density at 450 nm was read with a microplate reader (Molecular Devices).

Cholesterol depletion and sequestration

HUVECs were washed in the isotonic medium in which they were cultured, but without serum or antibiotics, then incubated in the same medium containing 10 mg/mL methyl-β-cyclodextrin (MβCD) or α-cyclodextrin (αCD; Sigma-Aldrich), an inactive analog of MβCB, for 15 minutes at 37°C[11] before exposing to shear stress in the flow chamber. To sequester cholesterol, filipin III (1 μg/mL; Sigma-Aldrich) was incubated with HUVECs in serum–free medium for 1 hour at 37°C before perfusion assays.

Disruption of clathrin-dependent endocytosis

We used 2 approaches to disrupt clathrin-mediated endocytosis. In some experiments, HUVECs were washed to remove serum and incubated for 1 hour at 37°C in Medium 199 containing 5 μg/mL chlorpromazine (Sigma-Aldrich) before perfusion assays. Alternatively, HUVECs were washed and incubated for 30 minutes at 37°C in Medium 199 supplemented with 0.45M sucrose (hypertonic medium) before the experiments.

Caveolin-1 knockdown

Caveolin-1 gene (GenBank Accession No. NM001753) silencing was performed using a mix of 2 siRNA duplexes (Integrated DNA Technologies): 1. 5′-GUUGUUGGGCUUGUAGAUGTT-3′, 3′-TTCAACAAC-CCGAACAUCUAC-5′, 2. 5′-AACUGUGUGUCCCUUCUGGTT-3′, and 3′-TTUUGACACACAGGGAAGACC-5′.

HUVECs were transfected with caveolin-1 or control (green fluorescent protein, Amaxa) siRNA (150 pmol/T25 flask) using a Nucleofector device (Amaxa) and HUVEC nucleofection solution (Lonza). Seventy-two hours after transfection, cells were collected and lysed with Laemmli sample buffer (Bio-Rad) for Western blotting with anti–human caveolin-1 and anti–β-actin. Band intensities corresponding to caveolin-1 were quantified using ImageJ software Version 134S. Alternatively, transfected cells were seeded in 24-well plates or 35-mm tissue-culture dishes, cultured for 72 hours to confluence, and used for VWF cell-surface enzyme-linked immunosorbent assay (ELISA) or perfusion assays, respectively.

StxB-induced thrombotic microangiopathy in mice

Adamts13$^{-/-}$ C57BL/6J mice[5] were crossed with CAST/Ei mice (The Jackson Laboratory). Studies in mice were performed under protocols approved by the University of Iowa institutional animal care and use committee. The *Adamts13*$^{+/-}$ progeny were identified by polymerase chain reaction genotyping,[5] backcrossed with CAST/Ei mice for at least 7 generations, and mated to yield *Adamts13*$^{-/-}$ and *Adamts13*$^{+/-}$ littermates in the CAST/Ei background. Recombinant Stx2B was administered intravenously. Complete blood counts and reticulocyte counts were performed[5] before treatment and for up to 8 days thereafter. Peripheral blood films were prepared by standard techniques.[5] Relevant normal values for this strain are: platelets approximately 1.5 million/μL, hemoglobin approximately 13 g/dL, and reticulocyte count < 4%.
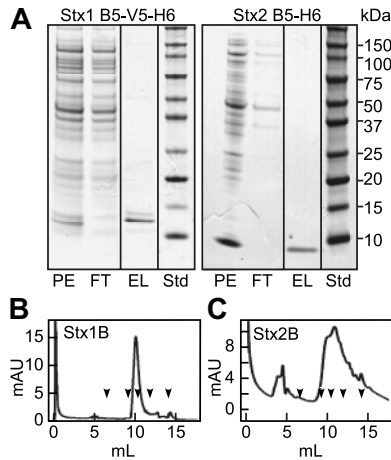
Figure 1. Recombinant Stx1B and Stx2B. Periplasmic extracts (PE) were prepared from *Escherichia coli* (*E coli*) BL21(DE3) expressing Stx1B subunit with C-terminal V5 and (His)$_6$ tags (left), or Stx2B subunit with a C-terminal (His)$_6$ tag (right). Extracts were chromatographed on HisPur Cobalt resin (Pierce) and eluted with buffer containing 0.15M imidazole. (A) SDS-PAGE of fractions and standard proteins (Std). StxB subunits were depleted from the flow through (FT) fractions and recovered as pure proteins in the eluate (EL). Purified Stx1B (B) and Stx2B (C) were analyzed TSK G3000SW gel filtration chromatography. The arrows indicate the elution positions, left to right, of thyroglobulin (670 kDa), IgG (158 kDa), ovalbumin (44 kDa), myoglobin (17 kDa), and vitamin B12 (1.35 kDa).

Results

Stx B pentamers stimulate the acute secretion of VWF from human endothelial cells

Stx1 and Stx2 holotoxins are known to activate human endothelial cells and cause the formation of VWF-platelet complexes that adhere to the cell surface.[4] As expected, we confirmed this reported activity of Stx1 and Stx2 holotoxins. However, we unexpectedly found that the recombinant StxB subunits also stimulate the acute secretion of VWF multimers We purified recombinant Stx1B and Stx2B from the periplasmic fraction of transformed *E coli* BL21, and when analyzed by gel filtration chromatography both preparations exhibited retention times similar to ovalbumin (44 kDa), consistent with a mainly pentameric structure. (Figure 1). HUVECs perfused with Stx1B or Stx2B secreted long strings of VWF that remained associated with the cell surface (Figure 2). Secretion was maximal within 5 minutes. Quantification from multiple images showed that Stx1B and Stx2B are at least as potent
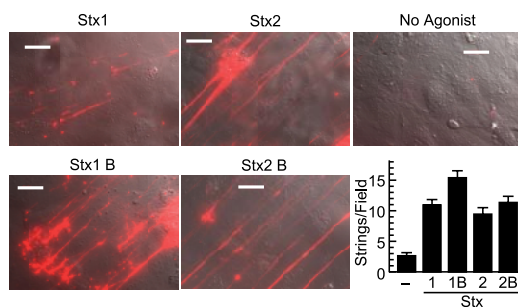
Figure 2. Stx1B and Stx2B induce secretion of VWF strings from cultured HUVECs. human umbilical vein endothelial cells (HUVECs) were perfused in a parallel plate flow chamber at a shear stress of 2.5 dyn/cm² for 10 minutes with fluorescent anti–von Willebrand Factor (anti-VWF) antibody and the indicated agonist (200 ng/mL). VWF strings were counted in 10 fields and values shown as mean ± SE. Scale bars are 10 μm. Experiments were conducted at least 3 times with similar results.
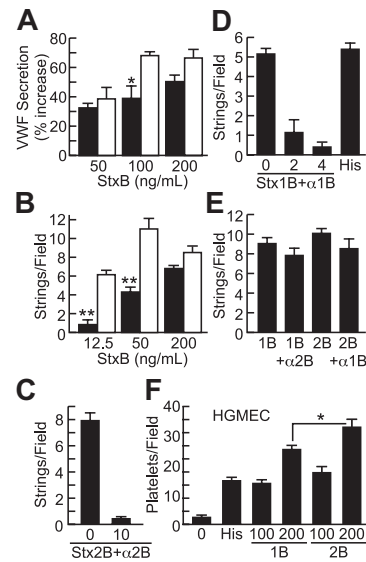

Figure 3. Stx1B and Stx2B induce endothelial VWF secretion and platelet adhesion in a dose-dependent and -specific manner. VWF deposition on HUVECs in response to Stx1B (■) or Stx2B (□) was tested under static conditions (A) and under laminar flow (B). VWF secretion was inhibited by preincubating Stx2B with anti-Stx2B monoclonal antibody 5H8 (10 μg/mL; C), or by preincubating Stx1B with polyclonal anti-Stx1B antiserum (2 or 4 μL/mL; D); anti-Stx2B did not inhibit Stx1B, and anti-Stx1B did not inhibit Stx2B (E). (F) Stx1B and Stx2B (ng/mL) induced platelet adhesion to HGMECs. Experiments were repeated at least 2 (C-F) or 3 times (A-B) with similar results. Values are shown as mean ± SE. Indicated comparisons of Stx1B and Stx2B are significant at $P < .05$ (*) or $P < .01$ (**) by Student *t* test.

as their holotoxin counterparts. Therefore, the ribotoxic Stx A subunit is not required for acute endothelial activation and VWF exocytosis.

We compared the efficacy of recombinant Stx1B and Stx2B in stimulating VWF secretion from HUVECs using 2 approaches. A cell-surface ELISA was used to quantify surface associated VWF under static conditions, and perfusion assays were performed to quantify VWF strings attached to HUVECs under laminar flow. In both assays, HUVECs responded to Stx1B and Stx2B in a dose-dependent manner, and Stx2B was more potent than Stx1B in causing acute VWF secretion (Figure 3A-B). In these experiments, the Stx1B had both V5 and His$_6$ epitope tags, whereas the Stx2B had only a His$_6$ tag (Figure 1). To exclude the possibility that these differences account for the greater potency of Stx2B, we performed a similar dose-response experiment with Stx1B and Stx2B that have identical His$_6$ tags and confirmed that Stx2B is more potent that Stx1B for inducing VWF secretion by HUVECs (supplemental Figure 1, available on the *Blood* Web site; see the Supplemental Materials link at the top of the online article). Interestingly, Stx1B or Stx2B concentrations greater than approximately 200 ng/mL were less effective (supplemental Figure 2), suggesting that excess StxB may prevent the optimal multivalent engagement of Gb3 on the cell surface.

Stx1B (0.2 μg/mL) and histamine (100μM) had comparable activity (Figure 3D). VWF secretion was inhibited by pretreatment of Stx1B with polyclonal anti-Stx1B[8] (Figure 3D) or by pretreatment of Stx2B with monoclonal anti-Stx2B antibody 5H8[9] (Figure 3C). Anti-Stx1B antibody did not inhibit Stx2B-induced VWF secretion, and anti-Stx2B antibody did not inhibit Stx1B-induced VWF secretion (Figure 3E).

HGMECs are derived from the kidney, a major target organ of HUS. Because HGMECs did not attach firmly enough to glass coverslips for reliable assays of VWF strings, we assessed platelet binding to secreted VWF on the surface of HGMECs grown in
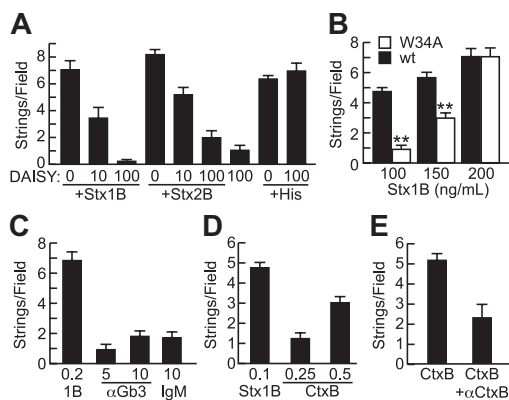
Figure 4. Specificity of StxB- and CtxB-induced VWF secretion. (A) Gb3 analog DAISY (μg/mL) was incubated with Stx1B, Stx2B (200 ng/mL), or histamine (100μM) before perfusion of HUVECs and quantification of VWF strings. (B) Wild-type Stx1B (■) and Stx1B W34A (□) were compared for ability to induce VWF string formation by HUVECs. Indicated comparisons between wild-type (wt) and W34A Stx1B are significant at $P < .01$ (**) by Student t test. (C) VWF string formation on HUVECs was assessed in response to recombinant Stx1B, anti-Gb3 IgM, or control mouse IgMκ antibody (Sigma-Aldrich); concentrations are in units of micrograms per milliliter. (D) VWF string formation on HUVECs in response Stx1B and CtxB at the indicated concentrations (μg/mL). (E) VWF string formation on HUVECs in response to CtxB (0.5 μg/mL) without or with anti-CtxB antibody (1 μg/mL). Experiments were performed at least 3 times with similar results. Values are shown as mean ± SE.

35-mm tissue culture dishes, to which they adhere more firmly. Recombinant B subunits from either Stx1 or Stx2 promoted platelet adhesion to HGMECs (Figure 3F). StxB-induced platelet adhesion was completely inhibited by monoclonal anti–glycoprotein Ibα (GPIbα) antibody 6D1, indicating dependence on platelet GPIbα (data not shown). At 200 ng/mL, Stx2B was consistently more potent than Stx1B (Figure 3F). In the experiment shown, Stx1B was more potent that histamine (100μM), but the relative potency of Stx1B and histamine varied between experiments with HGMECs.

Clustering of Gb3 is necessary to induce endothelial VWF secretion

DAISY is a carbohydrate–based multivalent Gb3 analog that binds Stx1 and Stx2 and protects mice from Stx intoxication.[11] Preincubation with DAISY blocked VWF secretion induced by Stx1B or Stx2B in a dose-dependent manner (Figure 4A). DAISY alone did not activate endothelial, nor did it inhibit histamine–induced VWF secretion (Figure 4A), providing evidence for specificity. These results indicate that the acute effect of StxB on endothelial cells depends on binding to cell-surface Gb3.

Crystallographic studies show that each Stx1B subunit has 3 binding sites for the terminal P[k] trisaccharide of Gb3, Galα(1,4)Galβ(1,4)Glcβ. Stx1B with a W34A mutation in site 3 binds with substantially decreased affinity to Gb3 in liposomes[12] and has decreased ability to induce membrane curvature and tubular invagination upon binding to HeLa cells or giant unilamellar vesicles containing Gb3.[13] When tested for ability to induce endothelial VWF secretion, Stx1B W34A was less effective than wild-type Stx1B for stimulating endothelial VWF secretion, although this difference was overcome at higher concentrations of Stx1B W34A (Figure 4B). VWF string formation induced by Stx1B W34A was also inhibited by DAISY (data not shown). Thus, optimal StxB-induced VWF secretion depends on high-affinity multivalent binding to membrane Gb3. However, treating HUVECs with pentavalent mouse monoclonal anti-Gb3 IgM did not induce VWF secretion, suggesting that Gb3 clustering is not sufficient (Figure 4C).
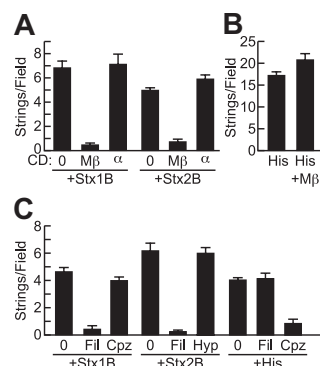
Figure 5. StxB-induced VWF secretion requires cholesterol but not clathrin. (A) HUVECs were incubated without (0) or with 10 mg/mL methyl-β-cyclodextrin (Mβ) or α-cyclodextrin (α) for 15 minutes at 37°C before perfusion with Stx1B or Stx2B (200 ng/mL; A) or histamine (100μM; B) and quantification of VWF strings. (C) HUVECs were preincubated without or with 1 μg/mL filipin (Fil) or 5 μg/mL chlorpromazine (Cpz) for 1 hour at 37°C, or with hypertonic medium containing 0.45M sucrose (Hyp) for 30 minutes at 37°C, perfused with Stx1B or Stx2B (200 ng/mL), and VWF strings were quantified. These experiments were conducted 3 times with similar results. Values are shown as mean ± SE.

Effects of cholera toxin on endothelial VWF secretion

Like Stx, cholera toxin (Ctx) is an AB5 toxin, but Ctx binds to ganglioside GM1. GM1 and Gb3 colocalize in lipid rafts,[14] and we find that CtxB also stimulates the secretion of VWF from HUVECs in a dose-dependent and specific manner (Figures 4D-E). CtxB is not as potent as Stx1B, possibly because the level of GM1 is much lower than that of Gb3 in endothelial membranes.[15]

Stx1B and Stx2B-induced VWF secretion depends on cholesterol but not clathrin

Pretreatment of HUVECs with MβCD, which reversibly disrupts lipid rafts by extracting cholesterol from the cell membrane,[16] inhibited StxB-induced VWF string formation on endothelial cells by more than 90%, whereas αCD, an inactive analog of MβCD, had no effect (Figure 5A). In addition, VWF string formation induced by Stx1B and Stx2B was prevented by treatment of HUVECs with filipin, which binds cholesterol and disrupts the structure and function of membrane microdomains[17] (Figure 5C). Histamine induced VWF secretion was not affected by cholesterol depletion with MβCD (Figure 5B) or by filipin (data not shown).

Stx can enter cells via both clathrin-dependent and independent mechanisms.[18,19] Disruption of clathrin with chlorpromazine did not affect VWF string formation on HUVECs induced by Stx1B (Figure 5C) or Stx2B (data not shown). Chlorpromazine is also an H1 histamine receptor antagonist,[20] and as expected chlorpromazine did inhibit histamine stimulated VWF release (Figure 5C). Similarly, inhibition of clathrin-dependent endocytosis with hypertonic medium[21] had no effect on VWF secretion induced by Stx1B (data not shown) or Stx2B (Figure 5C). Therefore cholesterol rich lipid rafts, but not clathrin, are required for StxB to induce endothelial VWF secretion.

StxB-induced VWF secretion is reduced by endothelial caveolin-1 knockdown

Because caveolae represent a subset of lipid rafts that are particularly abundant in endothelial cells, we tested whether StxB-induced VWF secretion depends on the level of caveolin-1, which is required for the structure of caveolae. Compared with mock transfection or treatment with control siRNA, HUVECs
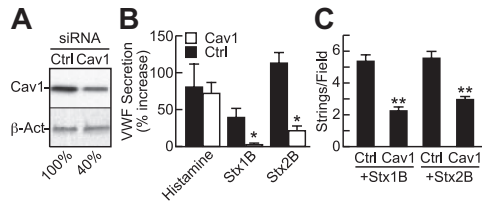
Figure 6. StxB-induced VWF secretion is reduced upon caveolin-1 knockdown. HUVECs were transfected with siRNA for caveolin-1 (Cav1), or green fluorescent protein (Ctrl). At 72 hours, (A) caveolin-1 (Cav1) and β-actin (β-Act) were detected in cell lysates by Western blotting with monoclonal anti–caveolin-1 (BD Biosciences) or anti–β-actin (AC-15; Sigma-Aldrich), normalizing band densities for Cav1 to β-actin for comparison to the mock condition (100%); or (B) the cells were treated under static conditions with histamine (100μM), Stx1B or Stx2B (200 ng/mL) and secreted cell-surface VWF assayed by cell-surface ELISA; or (C) cells were perfused with Stx1B or Stx2B and VWF strings were quantified. Indicated comparisons between Ctrl and Cav1 siRNA are significant at $P < .05$ (*) or $P < .01$ (**) by Student t test. These experiments were performed at least 3 times with similar results. Values are shown as mean ± SE.

transfected with caveolin-1 siRNA expressed approximately 60% less caveolin-1 (Figure 6A), secreted less VWF (Figure 6B), and formed fewer VWF strings (Figure 6C) in response to Stx1B or Stx2B; the response to histamine was unaffected. These results indicate that caveolin-1 is involved in StxB stimulated VWF exocytosis.

Stx2B causes thrombotic microangiopathy in ADAMTS13-deficient mice

The activity of StxB subunits on HUVECs and HGMECs suggests that StxB-induced endothelial activation could cause thrombotic microangiopathy in susceptible animals. We tested this possibility by injecting purified, endotoxin–free Stx2B into *Adamts13*^{−/−} CAST/Ei mice and heterozygous littermates. Stx2B was chosen because Stx2-producing *E coli* cause the majority of human D[+]HUS. Complete blood counts, platelet counts and reticulocyte counts were performed before treatment and for up to 8 days thereafter. Normal values for this strain include a platelet count of approximately 1.5 million/μL, hemoglobin of 13 g/dL, and reticulocyte count < 4%.

Among 13 *Adamts13*^{−/−} mice, 5 developed anemia (hemoglobin decrease > 4 g/dL) and 5 developed thrombocytopenia (platelets decrease > 500 000/μL, or decrease > 50% from pretreatment value) within the first day after administration of Stx2B (Figure 7A). Blood samples showed red blood cell fragmentation and striking reticulocytosis (Figure 7B). The prompt development of hemolytic anemia and thrombocytopenia is consistent with the rapid time course of StxB-induced VWF secretion observed for cultured HUVECs. No reticulocytosis or red cell fragments were observed in *Adamts1*^{+/−} mice. The hemoglobin and platelet count were decreased in 1 *Adamts13*^{+/−} mice that expired during blood sampling. Thus, Stx2B can induce striking hemolysis and thrombocytopenia in mice that cannot regulate VWF-dependent microvascular thrombosis because they lack ADAMTS13.

Discussion

StxB subunits of Shiga-like toxins have been thought to function primarily to facilitate the entry of A subunit into target cells, which leads to apoptosis after several hours. However, our results show that StxB also induces the secretion of VWF from cultured human endothelial cells within 5 minutes, and rapidly causes thrombotic

microangiopathy in mice with an appropriate genetic background. These previously unrecognized activities of StxB suggest that, in addition to endothelial apoptosis caused by Stx A subunit, VWF mediated platelet adhesion induced by StxB may contribute to the pathogenesis of D[+]HUS. The results of a recent linkage analysis are consistent with this hypothesis: the risk of developing D[+]HUS was associated (odds ratio 3.08, $P < .001$) with expression of the platelet GPIbα 145M polymorphic variant, which has greater affinity for VWF than the more common GPIbα 145T variant.[22]

Stx1 and Stx2 both bind Gb3 and use the same mechanism to inactivate ribosomes. However, Stx2 causes D[+]HUS more often than does Stx1, and this difference has not been explained. Stx1B and Stx2B are 50%-60% identical in amino acid sequence, and crystal structures show that many nonconserved amino acid residues are exposed on the exterior surface[23] where they may affect interactions with distinct components on cell surfaces. For example, Stx1 and Stx2 have different affinities for Gb3 in lipid rafts.[24] Using human endothelial cells from 2 tissue sources, we find that Stx2B is also more potent than Stx1B in promoting VWF secretion (Figure 3), which suggests that differences in Stx-induced cell signaling may contribute to the greater virulence of *E coli* that express Stx2.

Stx1B and Stx2B induce VWF secretion by binding to cell-surface Gb3 (Figure 4A). StxB binding also causes Gb3 clustering,[13] but VWF secretion is not induced by polyvalent anti-Gb3 IgM (Figure 4C). Therefore, Gb3 ligation and clustering appear necessary but may not be sufficient to activate endothelial cells.

After binding to the cell surface, Stx is internalized and delivered by retrograde transport to the ER. The rapidity of Stx-induced VWF secretion is not compatible with the prolonged time course of retrograde transport, but endocytic machinery at the plasma membrane may nevertheless contribute. Both clathrin-dependent and clathrin-independent pathways have been shown to mediate the endocytosis of Stx.[25] However, Stx-induced VWF secretion was not affected by inhibition of clathrin-mediated endocytosis (Figure 5C). Instead, secretion was blocked by interventions that disrupt membrane rafts including the extraction or sequestration of cholesterol (Figure 5), or knockdown of caveolin-1 (Figure 6). Therefore, Stx signaling downstream of Gb3 binding may involve endocytosis through caveolae, which are abundant on endothelial cells and comprise a subset of membrane rafts that
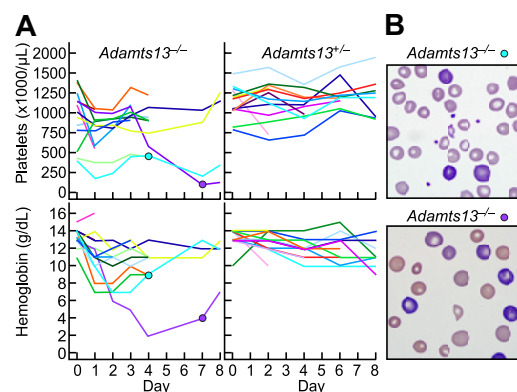
Figure 7. Stx2B induces thrombotic microangiopathy in *Adamts13*^{−/−} mice. Stx2B 1.25 ng/g body weight was injected intravenously into 13 *Adamts13*^{−/−} mice and 13 *Adamts13*^{+/−} mice. (A) Platelet counts and hemoglobin levels. (B) Blood films for the indicated mice at 4 days (top, reticulocytes 19%) or 7 days (bottom, reticulocytes > 50%) after injection with Stx2B, demonstrating red cell fragmentation and reticulocytosis.

participate in many physiological and pathological processes, such as atherosclerosis, hemostasis and thrombosis.[26,27]

The signaling pathways activated by StxB subunits remain to be characterized. Gb3 and other glycosphingolipids in membrane rafts such as GM1 associate with integrins,[28] growth factor receptors,[29] nonreceptor tyrosine kinases, heterotrimeric GTP-binding proteins and small GTPases.[30] Therefore, binding of StxB to Gb3 may induce VWF secretion by interacting with signaling molecules that cluster within membrane rafts or caveolae. For example, binding of Stx1B to Gb3-enriched membrane microdomains of renal tubular ACHN cells was reported to rapidly activate the Src family kinase Yes, which mediates cytoskeletal remodeling.[31,32]

Alternatively, StxB may activate cell signaling by mechanically deforming the plasma membrane.[13] Indeed, Stx1B has been shown to induce negative curvature and tubular invaginations in HeLa cells, mouse fibroblasts and model membranes. Although Stx B-induced tubule formation does not require caveolin-1,[13] depletion of caveolin-1 in HeLa cells markedly decreases the efficiency of tubule formation.[33] In addition, the W34A mutation in Stx1B impairs both membrane tubule formation[13] and VWF secretion (Figure 5). The homologous proteins polymerase I and transcript release factor, or cavin-1, and serum deprivation protein response, or cavin-2, are required for the biogenesis of caveolae, and these proteins also facilitate the recruitment of Stx B subunits to membrane tubules.[33] Components of these pathways could be considered as potential modifiers of the risk for developing D+HUS, either because they influence VWF-dependent microvascular thrombosis or because they affect other consequences of endothelial activation by StxB subunits.

Authorship

Contribution: J.H. designed and performed research, analyzed and interpreted data, and wrote the manuscript; D.G.M. performed research, analyzed and interpreted data, and wrote the manuscript; D.R.B. provided vital reagents; and J.E.S. designed research, analyzed and interpreted data, and wrote the manuscript.

Conflict-of-interest disclosure: J.E.S. has consulted for Baxter Innovations and Ablynx. The remaining authors declare no competing financial interests.

Correspondence: J. Evan Sadler, Department of Medicine, Washington University School of Medicine, 660 S Euclid Ave, Box 8125, St Louis, MO 63110; e-mail: esadler@wustl.edu.

References

1. Tarr PI, Gordon CA, Chandler WL. Shiga-toxin-producing Escherichia coli and haemolytic uraemic syndrome. *Lancet.* 2005;365(9464):1073-1086.

2. Garg AX, Suri RS, Barrowman N, et al. Long-term renal prognosis of diarrhea-associated hemolytic uremic syndrome: a systematic review, meta-analysis, and meta-regression. *JAMA.* 2003;290(10):1360-1370.

3. Mallard F, Antony C, Tenza D, Salamero J, Goud B, Johannes L. Direct pathway from early/recycling endosomes to the Golgi apparatus revealed through the study of shiga toxin B-fragment transport. *J Cell Biol.* 1998;143(4):973-990.

4. Nolasco LH, Turner NA, Bernardo A, et al. Hemolytic uremic syndrome-associated Shiga toxins promote endothelial-cell secretion and impair ADAMTS13 cleavage of unusually large von Willebrand factor multimers. *Blood.* 2005;106(13):4199-4209.

5. Motto DG, Chauhan AK, Zhu G, et al. Shiga-toxin triggers thrombotic thrombocytopenic purpura in genetically susceptible ADAMTS13-deficient mice. *J Clin Invest.* 2005;115(10):2752-2761.

6. Chauhan AK, Walsh MT, Zhu G, Ginsburg D, Wagner DD, Motto DG. The combined roles of ADAMTS13 and VWF in murine models of TTP, endotoxemia, and thrombosis. *Blood.* 2008;111(7):3452-3457.

7. Elliott SP, Yu M, Xu H, Haslam DB. Forssman synthetase expression results in diminished shiga toxin susceptibility: a role for glycolipids in determining host-microbe interactions. *Infect Immun.* 2003;71(11):6543-6552.

8. Zhao L, Haslam DB. A quantitative and highly sensitive luciferase-based assay for bacterial toxins that inhibit protein synthesis. *J Med Microbiol.* 2005;54(Pt 11):1023-1030.

9. Mukherjee J, Chios K, Fishwild D, et al. Human Stx2-specific monoclonal antibodies prevent systemic complications of Escherichia coli O157:H7 infection. *Infect Immun.* 2002;70(2):612-619.

10. Huang J, Roth R, Heuser JE, Sadler JE. Integrin alpha(v)beta(3) on human endothelial cells binds von Willebrand factor strings under fluid shear stress. *Blood.* 2009;113(7):1589-1597.

11. Mulvey GL, Marcato P, Kitov PI, Sadowska J, Bundle DR, Armstrong GD. Assessment in mice of the therapeutic potential of tailored, multivalent Shiga toxin carbohydrate ligands. *J Infect Dis.* 2003;187(4):640-649.

12. Soltyk AM, MacKenzie CR, Wolski VM, et al. A mutational analysis of the globotriaosylceramide-binding sites of verotoxin VT1. *J Biol Chem.* 2002;277(7):5351-5359.

13. Romer W, Berland L, Chambon V, et al. Shiga toxin induces tubular membrane invaginations for its uptake into cells. *Nature.* 2007;450(7170):670-675.

14. Kovbasnjuk O, Edidin M, Donowitz M. Role of lipid rafts in Shiga toxin 1 interaction with the apical surface of Caco-2 cells. *J Cell Sci.* 2001;114(Pt 22):4025-4031.

15. Muthing J, Duvar S, Heitmann D, et al. Isolation and structural characterization of glycosphingolipids of in vitro propagated human umbilical vein endothelial cells. *Glycobiology.* 1999;9(5):459-468.

16. Setiadi H, McEver RP. Clustering endothelial E-selectin in clathrin-coated pits and lipid rafts enhances leukocyte adhesion under flow. *Blood.* 2008;111(4):1989-1998.

17. Rothberg KG, Heuser JE, Donzell WC, Ying YS, Glenney JR, Anderson RG. Caveolin, a protein component of caveolae membrane coats. *Cell.* 1992;68(4):673-682.

18. Khine AA, Lingwood CA. Capping and receptor-mediated endocytosis of cell-bound verotoxin (Shiga-like toxin). 1: Chemical identification of an amino acid in the B subunit necessary for efficient receptor glycolipid binding and cellular internalization. *J Cell Physiol.* 1994;161(2):319-332.

19. Sandvig K, Olsnes S, Brown JE, Petersen OW, van Deurs B. Endocytosis from coated pits of Shiga toxin: a glycolipid-binding protein from Shigella dysenteriae 1. *J Cell Biol.* 1989;108(4):1331-1343.

20. Palacios M, Padron J, Glaria L, et al. Chlorpromazine inhibits both the constitutive nitric oxide synthase and the induction of nitric oxide synthase after LPS challenge. *Biochem Biophys Res Commun.* 1993;196(1):280-286.

21. Heuser JE, Anderson RG. Hypertonic media inhibit receptor-mediated endocytosis by blocking clathrin-coated pit formation. *J Cell Biol.* 1989;108(2):389-400.

22. Taranta A, Gianviti A, Palma A, et al. Genetic risk factors in typical haemolytic uraemic syndrome. *Nephrol Dial Transplant.* 2009;24(6):1851-1857.

23. Lee JE, Reed J, Shields MS, Spiegel KM, Farrell LD, Sheridan PP. Phylogenetic analysis of Shiga toxin 1 and Shiga toxin 2 genes associated with disease outbreaks. *BMC Microbiol.* 2007;4(7):109.

24. Tam P, Mahfoud R, Nutikka A, et al. Differential intracellular transport and binding of verotoxin 1 and verotoxin 2 to globotriaosylceramide-containing lipid assemblies. *J Cell Physiol.* 2008;216(3):750-763.

25. Schapiro FB, Lingwood C, Furuya W, Grinstein S. pH-independent retrograde targeting of glycolipids to the Golgi complex. *Am J Physiol.* 1998;274(2 Pt 1):C319-332.

26. Frank PG, Woodman SE, Park DS, Lisanti MP. Caveolin, caveolae, and endothelial cell function.

Arterioscler Thromb Vasc Biol. 2003;23(7):1161-1168.

27. Lopez JA, del Conde I, Shrimpton CN. Receptors, rafts, and microvesicles in thrombosis and inflammation. *J Thromb Haemost.* 2005;3(8): 1737-1744.

28. Lajoie P, Goetz JG, Dennis JW, Nabi IR. Lattices, rafts, and scaffolds: domain regulation of receptor signaling at the plasma membrane. *J Cell Biol.* 2009;185(3):381-385.

29. Ringerike T, Blystad FD, Levy FO, Madshus IH, Stang E. Cholesterol is important in control of EGF receptor kinase activity but EGF receptors are not concentrated in caveolae. *J Cell Sci.* 2002;115(Pt 6):1331-1340.

30. Razzaq TM, Ozegbe P, Jury EC, Sembi P, Blackwell NM, Kabouridis PS. Regulation of T-cell receptor signalling by membrane microdomains. *Immunology.* 2004;113(4):413-426.

31. Katagiri YU, Mori T, Nakajima H, et al. Activation of Src family kinase yes induced by Shiga toxin binding to globotriaosyl ceramide (Gb3/CD77) in low density, detergent-insoluble microdomains. *J Biol Chem.* 1999;274(49):35278-35282.

32. Takenouchi H, Kiyokawa N, Taguchi T, et al. Shiga toxin binding to globotriaosyl ceramide induces intracellular signals that mediate cytoskeleton remodeling in human renal carcinoma-derived cells. *J Cell Sci.* 2004;117(Pt 17):3911-3922.

33. Hansen CG, Bright NA, Howard G, Nichols BJ. SDPR induces membrane curvature and functions in the formation of caveolae. *Nat Cell Biol.* 2009;11(7):807-814.